

Accepted Manuscript

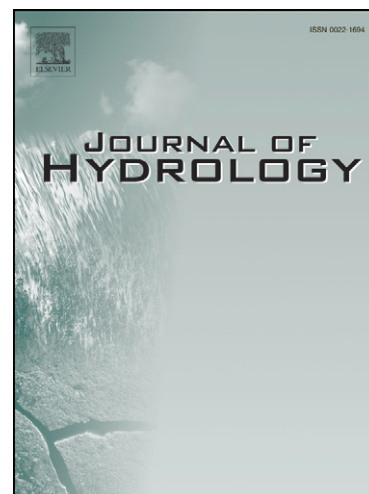
Pumping Test Analysis Using a Layered Cylindrical Grid Numerical Model in a Complex, Heterogeneous Chalk Aquifer

M.M. Mansour, A.G. Hughes, A.E.F. Spink, J. Riches

PII: S0022-1694(11)00100-4
DOI: [10.1016/j.jhydrol.2011.02.005](https://doi.org/10.1016/j.jhydrol.2011.02.005)
Reference: HYDROL 17509

To appear in: *Journal of Hydrology*

Received Date: 2 February 2010
Revised Date: 10 January 2011
Accepted Date: 3 February 2011



Please cite this article as: Mansour, M.M., Hughes, A.G., Spink, A.E.F., Riches, J., Pumping Test Analysis Using a Layered Cylindrical Grid Numerical Model in a Complex, Heterogeneous Chalk Aquifer, *Journal of Hydrology* (2011), doi: [10.1016/j.jhydrol.2011.02.005](https://doi.org/10.1016/j.jhydrol.2011.02.005)

This is a PDF file of an unedited manuscript that has been accepted for publication. As a service to our customers we are providing this early version of the manuscript. The manuscript will undergo copyediting, typesetting, and review of the resulting proof before it is published in its final form. Please note that during the production process errors may be discovered which could affect the content, and all legal disclaimers that apply to the journal pertain.

1 Title page:

2 **Pumping Test Analysis Using a Layered Cylindrical Grid Numerical**

3 **Model in a Complex, Heterogeneous Chalk Aquifer.**

4 M. M. Mansour, A. G. Hughes, A. E. F. Spink, J. Riches

5 **First author**

6 First name: Majdi

7 Middle Name: M

8 Last Name: Mansour

9 Academic degrees: BSc, MSc, PhD.

10 Affiliation: Senior Scientific Officer. British Geological Survey. Keyworth.

11 Nottingham. UK

12 Email: majm@bgs.ac.uk

13 Address: British Geological Survey

14 Kingsley Dunham Centre

15 Keyworth,

16 Nottingham, UK

17 NG12 5GG

18

19 **Contributing author 1**

20 First name: Andrew

21 Middle Name: G

22 Last Name: Hughes

23 Academic degrees: BSc, MSc, PhD.

24 Affiliation: Principal Scientist Officer. British Geological Survey. Keyworth.

25 Nottingham. UK

26 Email: aghug@bgs.ac.uk

27

28

29 **Contributing author 2**

30 First name: Andrew

31 Middle Name: E.F.

32 Last Name: Spink

33 Academic degrees: BSc, MSc, PhD.

34 Affiliation: Lecturer in Groundwater. The University of Birmingham.

35 Birmingham. UK

36 Email: a.e.f.spink@bham.ac.uk

37

38 **Contributing author 3**

39 First name: Jamie

40 Middle Name:

41 Last Name: Riches

42 Academic degrees: BSc, MSc.

43 Affiliation: Groundwater Resources Consultant. Thames Water. Reading. UK

44 Email: Jamie.Riches@thameswater.co.uk

45

46

47 **Pumping Test Analysis Using a Layered Cylindrical Grid Numerical**
48 **Model in a Complex, Heterogeneous Chalk Aquifer.**

49 M. M. Mansour, A. G. Hughes, A. E. F. Spink, J. Riches

50 **Abstract**

51 A groundwater investigation including several pumping tests has been carried out by
52 Thames Water Utilities Limited (TWUL) to improve the understanding of the
53 distribution of hydraulic properties of the Chalk in the Swanscombe area of Kent in
54 south-eastern England. The pumping test behaviour is complicated by: the fractured
55 condition of the Chalk, simultaneous pumping from adjacent boreholes, and variable
56 pumping rates during the test. In addition, the groundwater flow system is
57 complicated by quarrying of the Chalk. Analytical solutions for pumping test analysis
58 fail to represent these complex flow processes and cannot reproduce the observed
59 time drawdown curves. A layered cylindrical grid numerical model has been applied
60 to the results of the Swanscombe pumping test. This model can represent the
61 heterogeneity of the aquifer and the detailed flow processes close to the abstraction
62 borehole such as well storage, seepage face and well losses. It also includes a
63 numerical representation of the moving water table using a grid that deforms to
64 eliminate numerical instabilities. The analyses of the test results demonstrate that
65 they are significantly influenced by fracture flow, which needs to be included to
66 improve the simulation of the groundwater system; notwithstanding this, the layered
67 cylindrical grid numerical model reproduced many of the features in observed time-
68 drawdown, which allowed an assessment of the hydraulic characteristics of the
69 aquifer as well as the investigation of the impact of quarries on the test results. This
70 has demonstrated that the numerical model is a powerful tool that can be used to

71 analyse complex pumping tests and aid to improvement of the conceptual
72 understanding of a groundwater system.

73 **1.0 Introduction**

74 During the later part of 2002, a multiple borehole pumping test was conducted by
75 Thames Water Utilities Limited (TWUL) to understand the hydraulic properties of the
76 Chalk aquifer, in the Swanscombe area of Kent in south-eastern England, and to
77 assess abstraction sustainability (Fig. 1). Pumping tests are controlled field
78 experiments carried out to determine the hydraulic properties of an aquifer or to
79 validate a conceptual model of a groundwater system (BSI 1992). Such tests yield
80 plots of time-drawdown values which exhibit a behaviour dictated by the hydraulic
81 characteristics of the aquifer. Under ideal conditions, this behaviour can be
82 represented by analytical solutions to obtain the values of the hydraulic parameters of
83 the aquifer. Typical time-drawdown plots, produced by these analytical solutions,
84 have been described by a number of researchers, for example Neuman (1971, 1979),
85 Streltsova (1972, 1973), Gambolati (1976), and Kruseman and de Ridder (1990).

86 Previous studies of Chalk aquifer properties show that the transmissivity and storage
87 coefficient vary spatially depending on the geological development of the Chalk
88 (Allen et al. 1997). The development of fractures complicates the groundwater flow
89 behaviour and solution processes greatly affect the characteristics of the Chalk and the
90 flow mechanisms within it, which is often referred to as dual-porosity. It is, therefore,
91 anticipated that the hydraulic properties of the Chalk in the Swanscombe area will be
92 spatially variable, causing the time-drawdown curves to deviate from the typical plots.
93 This deviation is potentially exacerbated by: the existence of large active sub-water
94 table quarries (Fig. 2a); simultaneous abstraction from adjacent boreholes leading to
95 interfering cones of depression; and because of the occurrence of generator outages

96 causing random interruption to abstraction and unplanned periods of groundwater
97 head recovery. Consequently, the commonly used analytical solutions such as
98 Theis (1935) solution and the Cooper and Jacob (1946) approximation for analysing
99 pumping tests in confined aquifers, the Hantush-Jacob (1955) solution for leaky
100 aquifers, Boulton's (1954) model, Dagan's (1967) solution and Neuman's (1972)
101 equations for tests in unconfined aquifers cannot be applied effectively to the
102 Swanscombe pumping test. Other analytical solutions such as the analytical solution
103 for partially penetrating wells in unconfined aquifers (Neuman 1974) or (Moench
104 1993; 1994), the analytical solution that accounts for pumping from large diameter
105 wells in unconfined aquifers (Moench 1997), the solution for unsteady flows in
106 single-porosity or double-porosity confined aquifers (Barker 1988), etc. target specific
107 problems and cannot simulate the flow processes of this complex pumping test. A
108 numerical layered cylindrical grid model is applied to improve the conceptual
109 understanding of the system, especially the impact of quarries and to determine the
110 values of the hydraulic parameters of the Chalk aquifer. This paper demonstrates that
111 this numerical model is a flexible tool that can be applied to answer questions
112 imposed by the conceptual model, in this case the effect of quarries, and improves it.
113 It also demonstrates that despite the complexity of the Chalk groundwater system, the
114 numerical model can reproduce satisfactorily much of the behaviour of the observed
115 time-drawdown curves, allowing a better understanding of the aquifer hydraulic
116 characteristics.

117

118 **2.0 Materials and methods**

119 The Swanscombe area is located on the south-eastern side of the London Basin
120 (Fig 1). It comprises the main valley of the River Thames, bordered by wide terraces,
121 and Palaeogene age deposits over a Chalk plateau, which is terminated by an

122 escarpment to the south. The Chalk has a maximum thickness of approximately
123 200 m and is partly covered by Palaeogene deposits comprising the Lambeth Group
124 and the Thames Group. Along the Thames in the north of the area, the Chalk is
125 overlain by terrace deposits and riverine alluvium. The regional hydraulic gradient
126 slopes from the North Downs escarpment northwards towards the Thames. The area
127 is drained by the River Thames to the north, the Rivers Cray and Darent in the west
128 and the Rivers Ebbsfleet and Medway in the east. For further information about the
129 regional hydraulic gradient refer to Darling et al (2010).

130 Characteristic of the Swanscombe area is an abundance of raw materials that are
131 utilised by the cement industry: chalk, clay and alluvial deposits are worked and
132 gravel extraction is also common. Several sub-water-table quarries have been
133 abandoned as the costs of dewatering have exceeded the rewards from quarrying.
134 Other quarries are reaching their maximum development depth and, when they close,
135 pumping will cease. Two quarries in particular form the focus of this study; the
136 Eastern Quarry, which is ceased operating in late 2007 and the Western Quarry, which
137 has now been developed into a shopping centre.

138 The pumping test involved two abstraction wells plus four abstraction boreholes and
139 thirty-one observation boreholes (Fig. 2). The two abstraction wells, defined as such
140 on the basis of their large diameter size, are the Greenhithe abstraction well and the
141 Southfleet abstraction well. Greenhithe abstraction well is located near the north-
142 western corner of Eastern Quarry approximately 150 m from its western edge, and
143 Southfleet abstraction well is close to the Eastern Quarry and located approximately
144 550 m from its eastern side (Fig. 2a). These two pumping wells are approximately
145 2700 m apart. The four abstraction boreholes, defined as such on the basis of their
146 relatively small diameter size, are located in the area south of the quarries. These

147 boreholes are: Site A (the Western Bean Farm borehole), Site B (the West Drudgeon
 148 Farm borehole), Site C (the Mid Drudgeon Farm borehole) and Site D (the West
 149 Beacon Wood borehole). Of the four abstraction boreholes, Site A is closest to the
 150 Greenhithe well at a distance of 1800 m and Site C is the closest to Southfleet at a
 151 distance of 2000 m. A distance of approximately 1300 m separates Sites A and C.
 152 Pumping started on 18 October 2002 at sites A, B, and C with abstraction rates of
 153 19.0 l/s, 12.7 l/s and 77.5 l/s respectively. Abstraction at Site D started eight days
 154 later at a rate of 49.0 l/s. Abstraction at Greenhithe and Southfleet started 28 days
 155 later at rates of 46.0 l/s and 37.0 l/s respectively. The abstraction at all sites ceased on
 156 the 16 December 2002 and the recovery at the abstraction boreholes was recorded for
 157 a further two days. During the pumping phase, abstraction was interrupted randomly
 158 at all the sites either because of generator failures or for generator maintenance,
 159 leading to unplanned recovery periods. This paper focuses on the results obtained at
 160 Site C and two of its neighbouring observation boreholes, boreholes 12 and 19, to
 161 illustrate the complexity of the Chalk groundwater system and the advantages of using
 162 the numerical radial flow model to simulate this groundwater system and analyse the
 163 pumping test results. The observed drawdown results are shown in Figures 5 and 6.

164 **3.0 Theory/calculation**

165 The layered cylindrical grid numerical model uses the finite-difference method to
 166 solve the basic equation describing flow through a porous medium under confined and
 167 unconfined conditions. To simulate groundwater flow converging to a pumped well,
 168 the three-dimensional basic flow equation is written in cylindrical coordinates and the
 169 aquifer is discretised using a grid illustrated in Figure 3. For confined aquifers and in
 170 terms of the drawdown (s) this equation is given by (Rushton 2003):

$$171 \quad K_r \frac{\partial^2 s}{\partial r^2} + \frac{K_r}{r} \frac{\partial s}{\partial r} + \frac{K_\theta}{r^2} \frac{\partial^2 s}{\partial \theta^2} + \frac{K_z}{r^2} \frac{\partial^2 s}{\partial z^2} = S_s \frac{\partial s}{\partial t} + N \quad \text{Equation 1}$$

172 Where:

173 K_r, K_θ and K_z are the hydraulic conductivities in the radial, the
174 circumferential and the vertical directions respectively. (LT⁻¹)

175 S_s is the specific storage (L⁻¹)

176 N is an external source term. (T⁻¹)

177 r is the radius from the centre of the abstraction borehole to the point where
178 the drawdown s is calculated (L)

179 In a layered system, the head values of Equation 1 are averaged over the layer
180 saturated thickness and the horizontal hydraulic conductivity is replaced by the
181 transmissivity of the layer. This does not apply at the uppermost layer if the
182 groundwater system is under unconfined conditions. Under these conditions an
183 additional numerical layer is created at the top of the uppermost layer of the model to
184 represent the presence of the water table (Fig. 3).

185 The equation that describes the movement of the water table is discussed by Todsen
186 (1971) and Neuman (1972) and is given by:

$$187 \quad \frac{\partial \phi}{\partial t} = \frac{-1}{n_e} \left(K_r \frac{\partial s}{\partial r} \frac{\partial \phi}{\partial r} + \frac{K_\theta}{r^2} \frac{\partial s}{\partial \theta} \frac{\partial \phi}{\partial \theta} - K_z \frac{\partial s}{\partial z} \right) \quad \text{Equation 2}$$

188 Where:

189 ϕ is a function that represents the location of the water table and (L)

190 n_e is the porosity of the aquifer. (Dimensionless)

191 The complexity of this non-linear equation can be reduced by assuming that the
192 product of the hydraulic gradients is small and can be neglected (Rushton and

193 Redshaw 1979). In this case Equation 2 reduces to: $\frac{\partial \phi}{\partial t} = \frac{1}{S_y} \left(K_z \frac{\partial s}{\partial z} \right)$ where the

194 porosity is considered to be approximately equal to the specific yield S_y . By changing

195 the subject, this equation can be written as: $K_z \frac{\partial s}{\partial z} = S_y \frac{\partial \varphi}{\partial t}$ and then by Darcy's law:

196 $q_z = S_y \frac{\partial \varphi}{\partial t}$, allowing the term q_z to be added to the right hand side of Equation 1,

197 which is then applied only to the water table nodes. The radial interval between nodes

198 increases in a logarithmic pattern from the centre of the abstraction borehole where

199 the numerical grid is centred to the outer boundary. This creates a large number of

200 nodes close to the abstraction well and improves the representation of the steep

201 hydraulic gradient as a result of pumping in the vicinity of the abstraction borehole.

202 In contrast to a general saturated aquifer node, a water table node changes its location

203 vertically based on its head value calculated at the end of a time step (Fig. 3). This

204 allows the aquifer to dewater as the water table moves downwards and the saturated

205 thickness of the uppermost layer becomes spatially variable. The vertical flow

206 between nodes in different layers is determined by considering mass conservation at

207 the interface between layers.

208 To represent the water contained within the abstraction well, i.e. well storage, the

209 values storage coefficients of the nodes located inside the abstraction borehole and

210 where pumping is applied are all set to unity. The occurrence of the seepage face is

211 represented by acknowledging that the aquifer nodes located at the abstraction

212 borehole face became subject to atmospheric pressure when the water levels inside the

213 abstraction borehole drops below the base of their corresponding layers. When this

214 happens the groundwater head values of these nodes are fixed to a value equal to the

215 base elevations of their corresponding layers.

216 The model code has been developed in C++ programming language and benefits from

217 the object-oriented technology. Information on the application of this technology in

218 groundwater modelling can be found in the work of Spink et al. (2003) and

219 Jackson et al. (2003). For a full description of the model and its application refer to
220 Mansour (2003) and Mansour et al. (2003). This type of model is preferred to the
221 Cartesian grid groundwater models that allow grid refinement such as ZOOMQ3D
222 (Jackson et al. 2003) and MODFLOW 2005 (Harbaugh 2005) because of its better
223 representation of the flow processes taking place next to the abstraction borehole, e.g.
224 well losses, well storage, seepage face, etc. In addition, although the Cartesian grid
225 models yield accurate solutions at the observation boreholes, the solution at the
226 abstraction borehole is less accurate. The inaccuracy at the abstraction borehole is
227 primarily due to the structure of the Cartesian numerical grid, which does not allow
228 the specification of nodes at the well face and consequently it is not possible to set the
229 hydraulic conductance values between the node inside the well and its surrounding
230 aquifer nodes correctly. In addition, it is not possible to set both the area and the
231 perimeter of a rectangular cell in a Cartesian model to be equal to the area and
232 perimeter of the actual circular abstraction borehole at the same time. If the numerical
233 grid is refined so that the area of the rectangular cell is equal to the area of the
234 abstraction borehole the rectangular cell will have a perimeter that is smaller than the
235 actual borehole perimeter. As the area through which groundwater is flowing from
236 the aquifer to the abstraction borehole in the numerical model is smaller than in
237 reality, it causes the simulated drawdown to be greater than the observed one.

238 The preprocessor, RADMOD (Reilly and Harbaugh 1993), has been developed for
239 MODFLOW (McDonald and Harbaugh 1988) to simulate axi-symmetric flow to a
240 well. The radial flow model reported here has the advantage of simulating the moving
241 water table, which cannot be done in RADMOD.

242

243 **4.0 Results and discussion**

244 **4.1 Conceptual model**

245 The Chalk aquifer is partly overlain by Palaeogene strata in the Swanscombe area
246 (Fig. 1 and Fig. 2). However, the water table is within the Chalk Formation almost
247 everywhere and the Chalk is the only source of groundwater available for abstraction.

248 While groundwater flow in the Chalk is complicated by the presence of fractures or
249 high conductivity zones as demonstrated in the analysis of an earlier individual
250 pumping test (Spink and Mansour 2003), it has not been possible to determine the
251 size, extents, and directions of these high conductivity zones. Consequently, these
252 zones cannot be represented in details in the conceptual model and the Chalk aquifer
253 is represented here using two uniform hydro-geological layers. The upper one, in
254 which the high conductivity zones are better developed, is in direct contact with the
255 abstraction borehole at Site C. The lower layer, which represents the remainder of the
256 Chalk and is less well developed, is also included as it may contribute to the total
257 water abstracted (Fig. 2b). Aquifer permeability values obtained from the analysis of
258 the pumping test are related, therefore, to both the Chalk matrix and the fractures or
259 high conductivity zones within it.

260 The layered cylindrical grid model can address conceptual complexities related to the
261 representation of flow processes next to the abstraction borehole, the variation of
262 pumping rates, and the simultaneous pumping from more than one borehole.

263 However, the effects of the quarries on the pumping test results are not fully
264 understood. The quarries may cause an increase in drawdown because of the reduced
265 aquifer thickness in the zone where the aquifer is missing and through which
266 groundwater flows are converging towards the abstraction well. Conversely, it may
267 be also possible that the water held in the topographical depressions on the surface of

268 these quarries provides the system with a source of water which compensates the
269 effects of the missing part of the aquifer. These two conceptual representations of the
270 quarries are investigated by the numerical model.

271

272 **4.2 Overview of the test results: preliminary assessment**

273 The time-drawdown curve of the first abstraction phase at Site C (Fig. 5 Phase 1) does
274 not show the typical unconfined behaviour because of the step increases in the
275 pumping rate at the start of the test. The typical behaviour of a time-drawdown curve
276 in unconfined aquifers, as explained by Kruseman and de Ridder (1990), has an 'S'
277 shape (Fig. 4a) when plotted on logarithmic axes. Each section of the S curve reflects
278 the changes in the dominant process occurring in the aquifer. At early times, the
279 abstracted water is released instantaneously from storage by the expansion of the
280 water and the compaction of the aquifer. The unconfined aquifer effectively behaves
281 as confined, but the time-drawdown curve may not match the Theis solution because
282 of well storage, which delays the start of drawdown at the observation boreholes
283 (Zone 1 of Fig. 4a). Once the water table starts falling, the quantity of water released
284 from specific yield (S_y) reduces the gradient of the intermediate-time segment and the
285 time-drawdown curve is comparable to that obtained from a leaky aquifer (Zone 2 of
286 Fig. 4a). In the third stage, the time-drawdown curve once again tends to conform to
287 a Theis curve based on storage due to S_y . At this time, the water table is the major
288 contributor to the water abstracted from the aquifer (Zone 3 of Fig. 4a).

289 When plotted on logarithmic time and linear drawdown axes, the time-drawdown
290 curve also takes a typical shape that can be divided into three segments. The first is a
291 straight line that matches the Theis solution, if well storage is small (last part of the
292 curve in Zone 1 of Fig. 4b). The second starts when the straight line changes gradient

293 and flattens indicating that storage from water table is contributing to the system. The
294 length of the second segment depends on the vertical hydraulic conductivity and the
295 specific yield of the aquifer (Zone 2 of Fig. 4b). The third segment starts when the
296 rate of drawdown increases again reflecting the fall of the water table (Zone 3 of
297 Fig. 4b).

298 The plot of the first abstraction phase at Site C (Fig. 5 Phase 1) also shows a delayed
299 increase in the drawdown values at the start of the test indicating the presence of a
300 significant source of water which is likely to be well storage. The time-drawdown
301 curves of the subsequent abstraction phases, however, show typical unconfined
302 behaviour but do not reflect the expected water table movement at later times. The
303 presence of a larger well storage component is evident in these phases and is reflected
304 by the delayed fall at the start of each phase. The field data collected during the
305 recovery phase (Fig. 5 Phase 7) show a delayed initial rise that is probably due to
306 problems in the measuring device and cannot be used to confirm this large well
307 storage.

308

309 **4.3 Numerical analysis**

310 Site C abstraction borehole diameter is 0.42 m, with a depth of 137 m. It is cased to a
311 depth of 75 m below the ground surface. A 43 m layer of Palaeogene deposits
312 overlies the Chalk at this site but the initial water level is recorded at a depth of
313 77.1 m from the ground surface indicating that the water table is not found within the
314 Palaeogene strata. The pumping borehole is open along its full saturated depth.

315 While the casing of the Site C abstraction borehole has a diameter of 0.42 m,
316 geophysical well logging (Buckley 2003) indicates that this borehole is larger than its
317 nominal size in the open section. Accordingly, the well diameter used in the model is

318 increased to 0.6 m, which is the average diameter shown by the borehole logs. The
319 first part of the Chalk aquifer, which is in direct contact with the abstraction well, is
320 approximately 60 m thick at this position (Fig. 2b). It is represented numerically by
321 four layers, the three uppermost layers are 10 m thick and the lower one is 30 m thick.
322 The narrow thicknesses of the first three layers allow the formation of the seepage
323 face at the abstraction borehole wall. The second, deeper Chalk layer, which is not in
324 contact with the abstraction borehole (Fig. 2b), is approximately 108 m thick and
325 represented in the model by one numerical layer.

326 A three dimensional model was built to improve the representation of the quarries and
327 to improve the locations of the abstraction and observation boreholes within the
328 model. In a single slice numerical model, i.e. assuming radial symmetry and
329 simulating groundwater flow using the radial and vertical directions only, observation
330 borehole 12 coincides with Site D abstraction borehole and observation borehole 17
331 coincides with Site B abstraction borehole. Consequently, it is not possible to
332 simulate the groundwater heads at the observation wells correctly as they coincide
333 with the abstraction boreholes. The three-dimensional numerical model is built by
334 replicating the vertical cross section described above fourteen times along different
335 radial directions. The 14 slices provided a line of nodes along the radial direction
336 next to the abstraction and observation boreholes of interest (Fig. 2a). In three-
337 dimensional view the numerical model takes a form that is similar to the one shown in
338 Figure 3 but without the well casing. While the groundwater flow processes at
339 borehole Site C are represented in detail, the remaining pumping boreholes are
340 included in the model by assigning the corresponding abstraction to the nearest model
341 node (Fig. 2a).

342 The model was calibrated by modifying the values of the aquifer hydraulic parameters
343 until the simulated drawdown curves match the observed ones. Many trial values for
344 the aquifer parameters were used to match the simulated and field time drawdown
345 curves. Commencing with parameter values suggested by previous studies of the
346 Chalk (Allen et al. 1997), each trial involved changing the value of one parameter,
347 based on the effects that this parameter has on the relevant time-drawdown curves.
348 The parameters modified are: the horizontal and vertical hydraulic conductivities, the
349 specific yield and the specific storage of each layer of the model. Possible values for
350 the different hydraulic parameters can be established from this trial and error exercise.
351 To improve the fit between the numerical and field results the parameter estimation
352 package PEST (Doherty 2004) was used. PEST is model-independent software that
353 modifies the input files of the model and adjusts a preselected set of its parameters
354 until the discrepancy between the field and numerical results are reduced to a
355 minimum. PEST undertakes many model runs to optimise the parameter values and
356 to perform uncertainty analysis. PEST was used here to refine the hydraulic
357 parameter values and to estimate the uncertainty associated with these values.
358 Initially PEST was used without the inclusion of the quarries in the numerical model.
359 The parameters modified by PEST were: the horizontal and vertical hydraulic
360 conductivities, the specific yield and the specific storage, and the well loss factor.
361 The values of the hydraulic parameters optimised by PEST, as well as the estimated
362 95% confidence limits, are given in Table 1. The optimised transmissivity value of
363 the part of the Chalk that is in direct contact with the borehole is $1340 \text{ m}^2 \text{ day}^{-1}$. The
364 optimised vertical hydraulic conductivity value is 0.86 m day^{-1} . The optimised
365 storage coefficient and specific yield are 1×10^{-5} and 0.012 respectively.

366 Subsequently, the quarries are added to the numerical model by altering the hydraulic
367 connections between the nodes to either remove the volume represented by the
368 quarries completely, or by reducing the thickness of the first layer of the Chalk, but
369 assuming that the water stored within the quarry is significant and is available to be
370 drawn by the abstraction boreholes. Two additional runs were undertaken to
371 represent these conditions. In the first run the quarries were included in the model by
372 introducing internal impermeable boundaries along the quarry walls in the uppermost
373 numerical layer (numerical link (H) in Figure 3). The nodes located within the quarry
374 area, however, remained connected to the nodes underneath them by the mean of the
375 vertical hydraulic conductivity (numerical links (V) in Figure 3). Simulated
376 drawdown values produced from this run did not show significant differences from
377 the results when the quarry is ignored, because the internal boundaries do not greatly
378 affect the results and the vertical hydraulic connection was enough to withdraw water
379 from the specific yield storage of the nodes located within the quarry area. In the
380 second run the vertical connections between the nodes located within the quarries and
381 the nodes underneath them were both disconnected (Fig. 3). This run assumed that
382 the quarried Chalk was absent. The simulated drawdown values were influenced by
383 the disconnection of the nodes within the quarries, especially at the end of the
384 abstraction phases. These are the results presented in Figures 5 and 6.

385 Figure 5 shows a comparison between the simulated and observed drawdown values
386 at the abstraction borehole C. The numerical model reproduced satisfactorily the
387 steps in the time-drawdown curve of the first abstraction phase. In addition, the
388 simulated drawdown values and the gradient of the time-drawdown curve from
389 0.01days follow the observed ones, indicating that the hydraulic parameters used in
390 the numerical model are representative to the overall hydraulic characteristics of the

391 aquifer. The slight drawdown observed at approximately one day was produced after
392 the inclusion of quarries in the numerical model. The delayed decline recorded in the
393 field data (Fig. 5 Phase 2) suggests the presence of a larger well storage component
394 than is evident in the other phases. The field data collected during the recovery phase
395 (Fig. 5 Phase 7) show a delayed initial rise, but this may be due to a problem with the
396 measuring device. However, the numerical results do show an acceptable level of
397 recovery compared to the field data when abstraction is interrupted in the fourth
398 abstraction phase (Fig. 5 Phase 4).

399 Many of the observation boreholes show little response to pumping at the abstraction
400 boreholes and some of the observation boreholes show fluctuations in groundwater
401 levels that cannot be related to the pumping test. The only time-drawdown curves that
402 show reasonable correlation to abstraction at Site C are those at Bean Farm borehole
403 and Eastern Drudgeon Farm borehole, which are situated approximately 920 m and
404 240 m away from abstraction borehole C (Boreholes 12 and 19 in Fig. 2a). The match
405 between the simulated and drawdown values of the first two abstraction phases is
406 acceptable, indicating that the hydraulic conductivity and the storage coefficient
407 values, which control the gradient of the time-drawdown curve and the start of
408 drawdown respectively, are representative of the hydraulic characteristics of the
409 aquifer (Fig. 6). The behaviour of the simulated time-drawdown curves over the
410 remaining abstraction phases is comparable to the observed ones, but there are vertical
411 shifts between them. This is caused by the sudden drop in drawdown values at the
412 end of the second abstraction phase and is particularly evident in the Eastern
413 Drudgeon Farm borehole. This behaviour can be caused by the presence of fractures
414 that dry up when the water table falls beneath them leading to significant change in
415 the transmissivity of the Chalk aquifer. Fractured or high conductivity zones can be

416 modelled using the layered cylindrical grid model. However, in this instance it was
417 decided to concentrate on the impact of the quarries on the groundwater system.

418

419 **5.0 Conclusion**

420 This paper discusses the analysis of a complex pumping test undertaken in the Chalk
421 aquifer of the Swanscombe area, south-east London, using a numerical layered
422 cylindrical grid model. The complexity of the Swanscombe pumping test arises from
423 factors such as abstraction from a partially penetrating abstraction borehole, the
424 stepwise increase of abstraction, the unplanned intermittent stoppages of pumping
425 during the test period and simultaneous pumping from adjacent boreholes. In
426 addition, the test results were affected by the presence of major quarries in the area.
427 Two scenarios are used to study the impact of the quarries on the test results. In the
428 first scenario, a quarry is represented in the model by imposing internal impermeable
429 boundaries along the locations of its walls whilst allowing the water stored within it to
430 contribute to the groundwater system. Quarries in this scenario did not impact the
431 simulated results. In the second scenario, in addition to the internal no flow
432 boundaries, the volume of water held by the quarries are completely removed from
433 the model. This quarry representation caused additional drawdown at the end of the
434 abstraction phases and improved the match between the observed and simulated time-
435 drawdown curves. This numerical configuration is used to estimate the hydraulic
436 parameter values of the aquifer.

437 The numerical results showed that a transmissivity value of $1340 \text{ m}^2 \text{ day}^{-1}$ of the part
438 of the Chalk that is in direct contact with the borehole, a vertical hydraulic
439 conductivity value of 0.86 m day^{-1} , and a storage coefficient and a specific yield of
440 $1 \times 10^{-5} \text{ m}^{-1}$ and 0.012 respectively produce a good match between the observed and

441 simulated time drawdown curves. The use of the numerical model permitted the
442 deployment of the parameter estimation software PEST (Doherty 2004) to optimise
443 the values of the hydraulic parameters and to undertake uncertainty analysis. It was
444 found that the highest uncertainty was associated with the value of the storage
445 coefficient with the 95% confidence limits being approximately 45% greater or
446 smaller than the estimated value. The second highest uncertainty is associated with
447 the values of the specific yield and vertical hydraulic conductivity with the 95%
448 confidence limits being approximately 25% greater or smaller than the estimated
449 values (Table 1). These values fall within the limits reported in the literature for Chalk
450 aquifers (see for example Allen et al., 1997) and can be used to specify the hydraulic
451 parameter values for this site in a regional Cartesian model.

452 This paper demonstrates that the layered cylindrical grid model used in this study can
453 incorporate enough mechanisms to reproduce the complex behaviour of the time-
454 drawdown curve and has many advantages on the use of conventional analytical
455 solutions and on the Cartesian models which are not designed to simulate
456 groundwater flow converging to a pumped borehole. This work also demonstrates that
457 the cylindrical grid numerical model is a powerful tool for analysing the pumping test
458 results. It provides useful information on both the well performance and the hydraulic
459 characteristics of the aquifer which helps improving the conceptual model of aquifers
460 such as the complex Chalk aquifer.

461

462

463

464

465

466

467

468

469

470

471

472

473

474

475

476

477

478

479

480

481

482

483

484

485

486

487

488

489

490 **References**

- 491 Allen, D.J., Brewerton, L.J., Colbey, L.M., Gibbs, B.R., Lewis, M.A., Macdonald, A.M.,
492 Wagstaff, S.J., Williams, A.T., 1997. The physical properties of major aquifers in England
493 and Wales. British Geological Survey Technical Report WD/97/34. Environment Agency R
494 & D Publication 8
- 495 Barker, J., 1988. A generalised radial-flow model for pumping tests in fractured rock. *Water*
496 *Resources Research*. 24, 10, 1796 – 1804.
- 497 Boulton, N.S., 1954. The drawdown of a water-table under non-steady conditions near a
498 pumped well in an unconfined formation. *Proceedings of the Institution of Civil Engineers*. 3,
499 Part 3, 564 – 579
- 500 BSI, 1992. Code of practice for Test pumping of water wells. BS 6316 : 1992. London, UK.
- 501 Buckley, D., 2003 Swanscombe Phase 2a Task 2.2 Geophysical Logging. British Geological
502 Survey Technical Report. CR/01/239C.
- 503 Cooper, H.H., Jacob, C.E., 1946. A generalized graphic method for evaluating formation
504 constants and summarizing well-field history. *Transactions of American Geophysical Union*.
505 27, 4, 526 – 534.
- 506 Dagan, G., 1967. Linearised solutions of free surface groundwater flow with uniform
507 recharge. *Journal of Geophysical Research*. 72, 4, 1183 – 1193.
- 508 Darling, W.G., Goody, D.C., Riches, J., Wallis, I., 2010. Using environmental tracers to
509 assess the extent of river-groundwater interaction in a quarried area of the English Chalk.
510 *Applied Geochemistry*. 25, 923 – 932.
- 511 Doherty, J., 2004. PEST: Model-independent parameter estimation user manual. Watermark
512 Numerical Computing
- 513 Gambolati, G., 1976. Transient free surface flow to a well: An analysis of theoretical
514 solutions. *Water Resources Research*. 12, 1, 27 – 39.

- 515 Hantush, M.S., Jacob, C.E., 1955. Non-Steady Radial Flow in an Infinite Leaky Aquifer.
516 Transactions of the American Geophysical Union. **36**, 95 – 100.
- 517 Harbaugh, A.W., 2005. MODFLOW 2005, The U.S. Geological Survey modular ground-
518 water model-the Ground-Water Flow Process: U.S. Geological Survey Techniques and
519 methods 6-16, variously p.
- 520 Kruseman, G.P., de Ridder, N.A., 1990. Analysis and evaluation of pumping test data. The
521 International Institute for Land Reclamation and Improvement. Publication 47.
- 522 Jackson, C.R., Hughes, A.G., Mansour, M.M., Spink, A.E.F., Bloomfield, J.P., Riches, J.,
523 Jones, M.A., 2003. Numerical modelling of a multiple-well pumping test using a locally
524 refined, object-oriented regional groundwater model. MODFLOW and More 2003:
525 Understanding through modelling, Conference Proceedings, Golden, CO, September 2003,
526 383 – 387.
- 527 Mansour, M.M., 2003. Flow to wells in unconfined aquifers using mesh refinement and
528 object-oriented technology. Ph.D. thesis. The University of Birmingham, UK.
- 529 Mansour, M.M., Spink, A.E.F., Riches, J., 2003. Numerical investigation of flow to pumped
530 wells in heterogeneous layered aquifers using radial flow models. MODFLOW and More
531 2003: Understanding through modelling, Conference Proceedings, Golden, CO, September
532 2003, 388 – 392.
- 533 McDonald, M.G., Harbaugh, A.W., 1988. A modular three-dimensional finite-difference
534 ground-water flow model. Technical report, U.S. Geol. Survey, Reston, VA.
- 535 Moench, A.F., 1993. Computation of type curves for flow to partially penetrating wells in
536 water-table aquifers. Ground Water, 31, 966 – 971.
- 537 Moench, A.F. 1994. Specific yield as determined by type-curve analysis of aquifer-test data.
538 Ground Water 6, 2, 37 – 46.

- 539 Moench, A.F. 1997. Flow to a well of finite diameter in a homogeneous, anisotropic water
540 table aquifer. *Water Resources Research*, 33, 6, 1397 – 1407.
- 541 Neuman, S.P., Witherspoon, P.A., 1971. Analysis of non-steady flow with a free surface
542 using the finite element method. *Water Resources Research*, 7, 3, 611 – 623.
- 543 Neuman, S.P., 1972. Theory of flow in unconfined aquifers considering delayed response of
544 the water table. *Water Resources Research*, 8, 4, 1031 – 1045.
- 545 Neuman, S.P., 1974. Effect of partial penetration on flow in unconfined aquifers considering
546 delayed gravity response. *Water Resources Research*, 10, 2, 303 – 312.
- 547 Neuman, S.P. 1979. Perspective on "delayed yield". *Water Resources Research*, 15, 899 –
548 908.
- 549 Reilly, T.E., Harbaugh, A.W., 1993. Simulation of cylindrical flow to a well using the U.S.
550 Geological Survey modular finite-difference groundwater flow model. *Ground Water*, 31, 3,
551 489 – 494.
- 552 Rushton, K.R., 2003. *Groundwater Hydrology. Conceptual and computational model.* John
553 Wiley and Sons Ltd, Chichester, UK.
- 554 Rushton, K.R., Redshaw, S.C., 1979. *Seepage and groundwater flow.* John Wiley and Sons,
555 Chichester, UK.
- 556 Streltsova, T.D. 1972. Unsteady radial flow in an unconfined aquifer. *Water Resources*
557 *Research*, 8, 4, 1059 – 1066.
- 558 Streltsova, T.D., 1973. Flow near a pumped well in an unconfined aquifer under nonsteady
559 conditions. *Water Resources Research*, 9, 1, 227 – 235.
- 560 Spink, A.E.F., Jackson, C.R., Hughes, A.G., Hulme, P.J., 2003. The benefits of object-
561 oriented modelling demonstrated through the development of a regional groundwater model.
562 MODFLOW and More 2003: Understanding through modelling, Conference Proceedings,
563 Golden, CO, September 2003, 336 – 340.

564 Spink, A.E.F., Mansour, M.M. 2003. Swanscombe Phase 2. Task 6: Preliminary Modelling.
565 Report prepared for the British Geological Survey. Wallingford, England.

566 Theis, C.V., 1935. The relation between the lowering of the piezometric surface and the rate
567 and duration of discharge of a well using groundwater storage. Transactions of the American
568 Geophysical Union, 16th annual meeting, 519 – 524.

569 Todsén, M., 1971. On the solution of transient free-surface problems in porous media by
570 finite-difference methods. Journal of Hydrology, 12, 177 – 210.

571
572
573
574
575
576
577
578
579
580
581
582
583
584
585
586
587
588

589

590

591 Figure 1: Regional setting of the Swanscombe area.

592 Figure 2: Conceptual model and numerical model setting at site C

593 Figure 3: Schematic representation of a multi-layered aquifer and the numerical

594 representation of quarries.

595

596 Figure 4: A typical time-drawdown curve obtained from pumping in unconfined

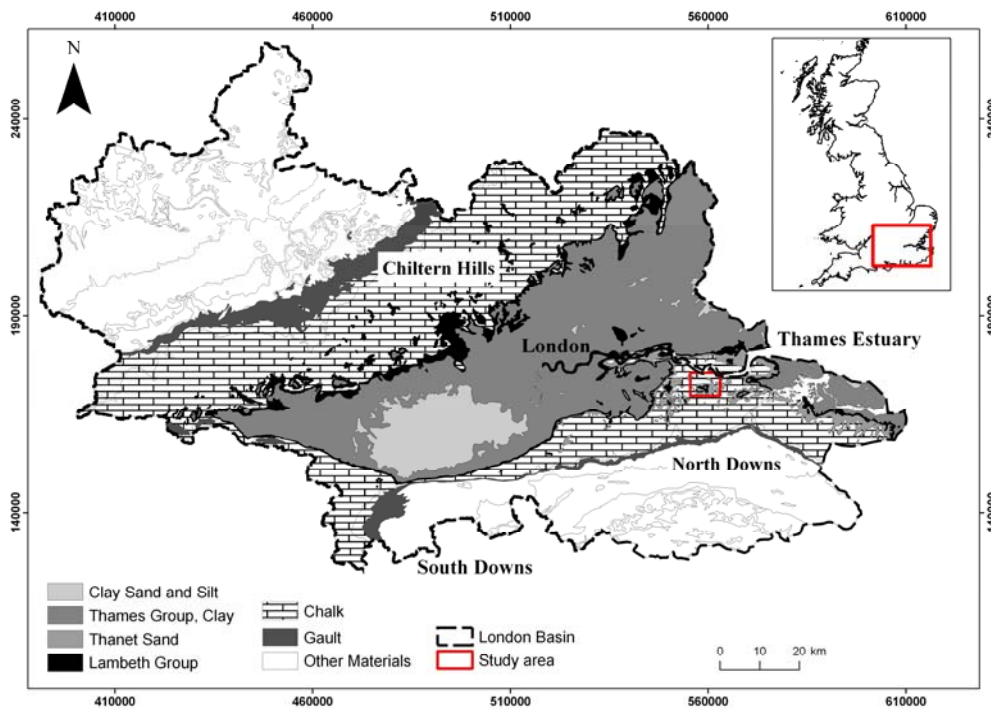
597 aquifers. (a): log-log scale. (b): log-arithmetic scale.

598 Figure 5: Field and numerical time-drawdown curves at Site C abstraction borehole

599 Figure 6: Field and numerical time-drawdown curves at Bean Farm and Eastern

600 Drudgeon Farm observation boreholes

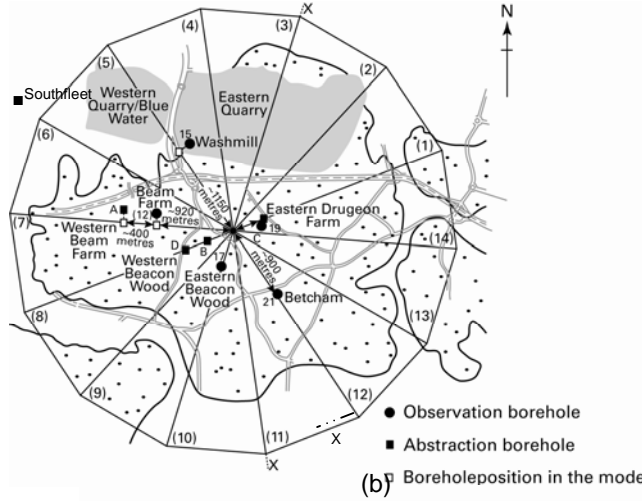
601 Table 1: Optimised hydraulic parameter values and the 95% confidence limits.



602

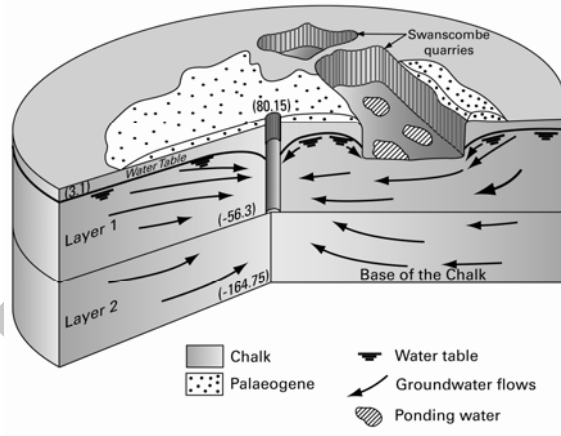
ACCEPTED MANUSCRIPT

Greenhithe



603

(a)



604

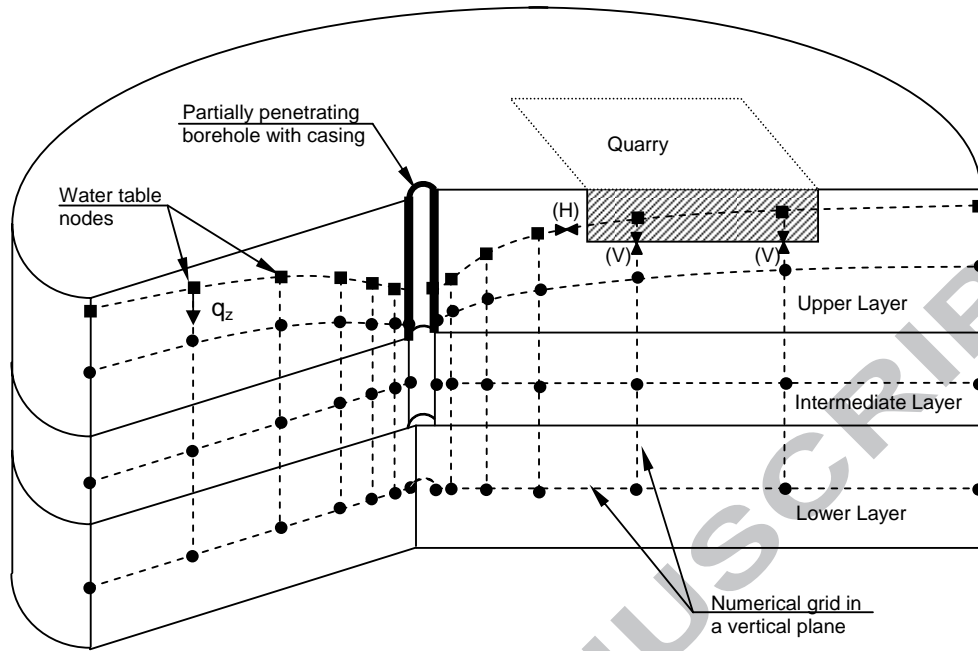
605

606

607

ACCEPTED

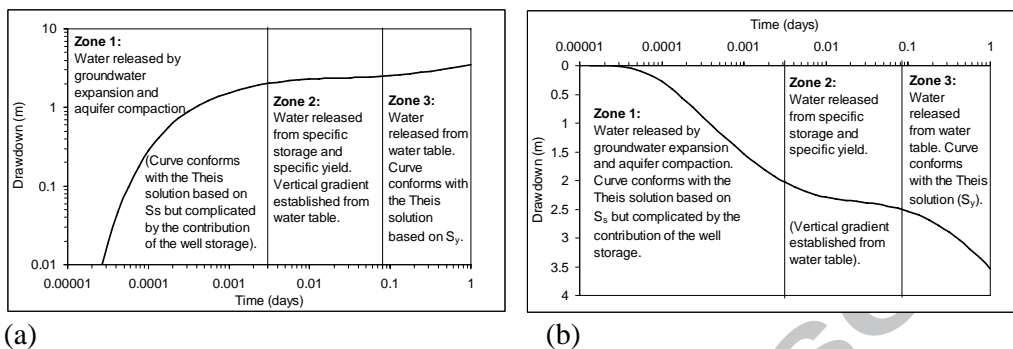
608



ACCEPTED MANUSCRIPT

609

610



611 (a)

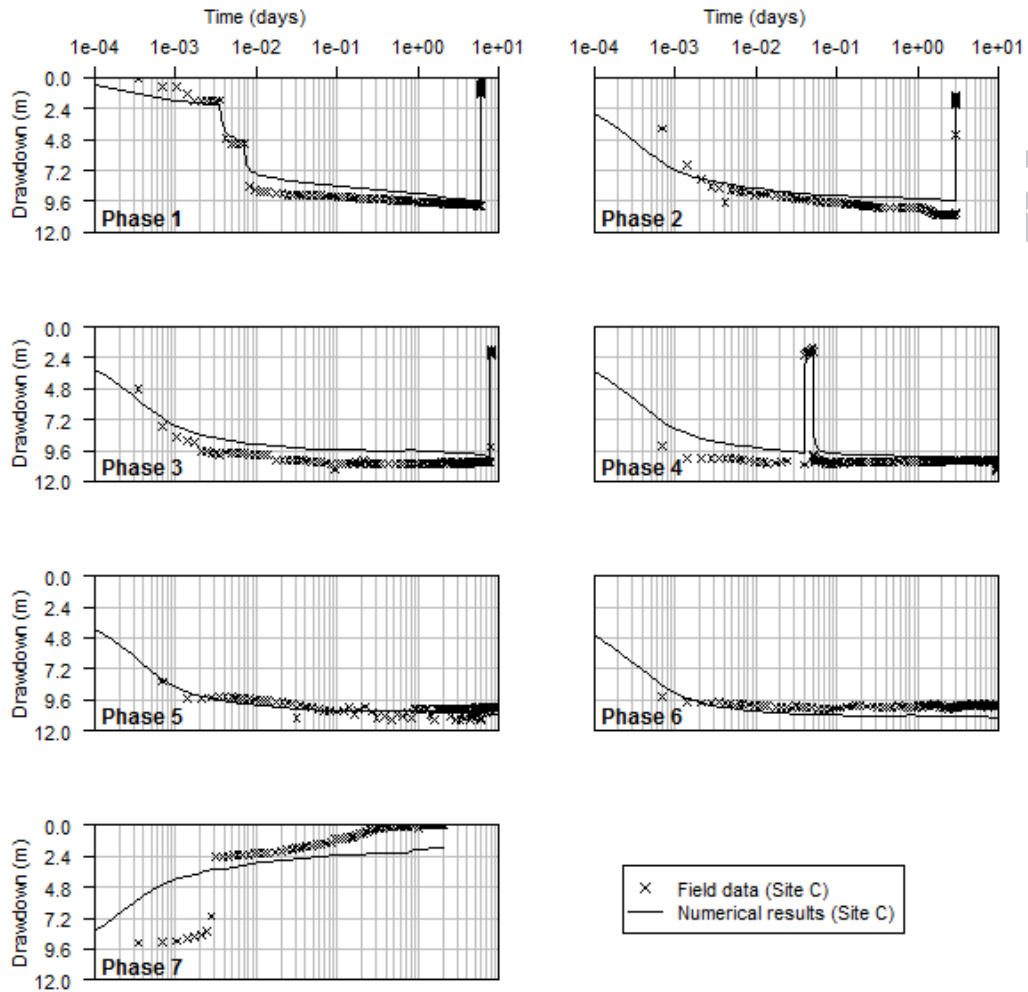
(b)

612 Figure 5: A typical time-drawdown curve obtained from pumping in unconfined

613 aquifers. (a): log-log scale. (b): log-arithmetic scale.

614 finite-difference methods. Journal of Hydrology, 12, pp 177–210

615



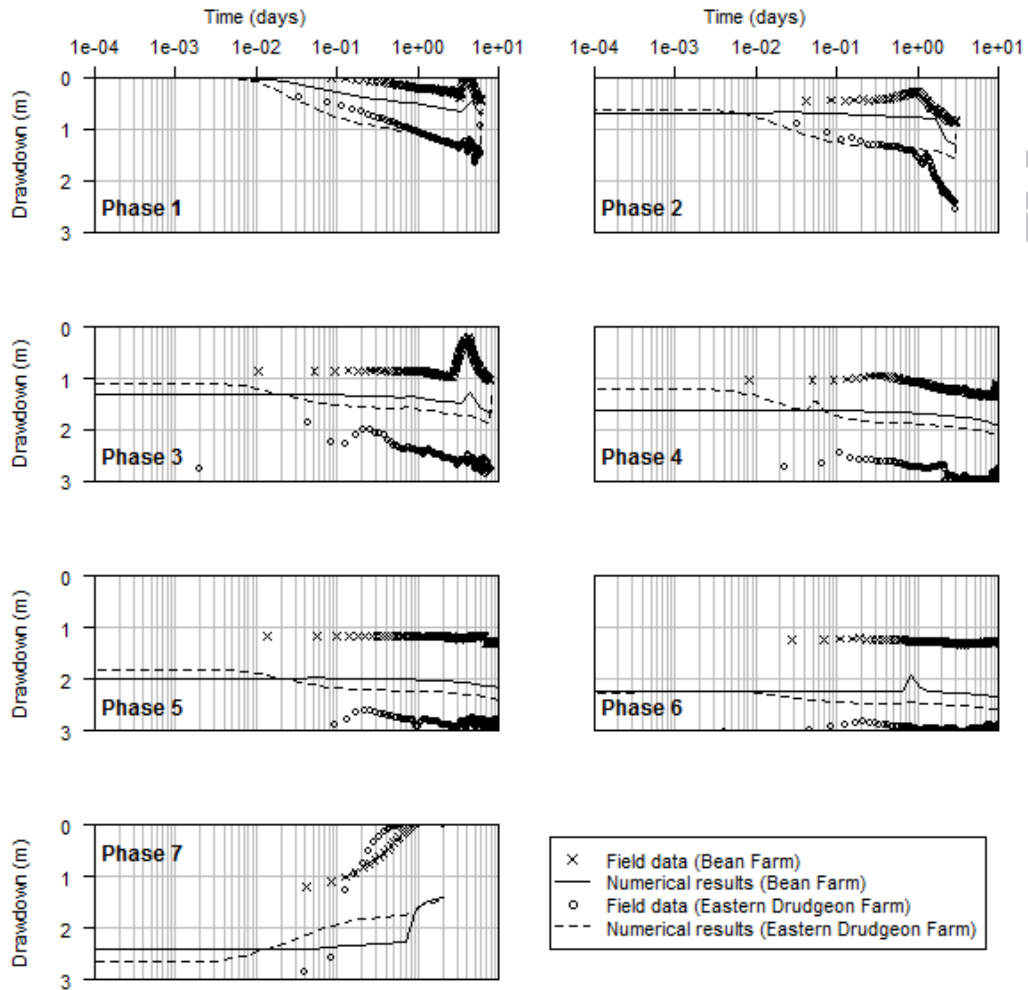
616

617

618

619

620



621

622

623

624

625

626

627

628

629

Parameter	Estimated value	95% confidence limits	
		Lower limit	Upper limit
Horizontal hydraulic conductivity K_h (m day ⁻¹)	22.33	20.5	24
Vertical hydraulic conductivity K_v (m day ⁻¹)	0.086	0.065	0.107
Specific storage S_s (m ⁻¹)	1e-05	5.5e-06	14.5e-5
Specific yield S_y (dimensionless)	0.012	0.0087	0.015
Well loss factor (dimensionless)	0.09	0.072	0.109

630

631 **Research highlights**

632

633 A layered cylindrical grid model is used to analyse pumping test results
634 conducted in a quarried Chalk aquifer.

635 Quarries did not show significant impact the results unless nodes they occupy
636 are completely disconnected.

637 Numerical model is a powerful tool to test conceptual ideas.

638 Numerical model produces useful information regarding the hydraulic
639 characteristics of the aquifer.

640

641

ACCEPTED MANUSCRIPT